DIRECT OBSERVATION OF THE STAGES OF LASER BREAKDOWN IN THE SAMPLES OF TRANSPARENT TARGETS IN THE TEMPORAL RANGE FROM FEMTO- TO NANOSECONDS

I.V. BLONSKYI,[1] V.M. KADAN,[1] O.I. SHPOTYUK,[2] I.A. PAVLOV[1]

[1]Institute of Physics, Nat. Acad. of Sci. of Ukraine
(46, Nauky Prosp., Kyiv 03650; e-mail: blon@iop.kiev.ua)

[2]Scientific Research Company "Karat"
(202, Stryiska Str., Lviv 79031; e-mail: shpotyuk@novas.lviv.ua)

PACS 42.65.Re; 42.65.Jx; 52.38.Dx

The main stages of a laser breakdown and accompanying phenomena have been investigated by the example of typical isotropic transparent media (K-8 optical glass and KU-1 fused silica) exposed to powerful femtosecond pulses. For this purpose, we created new techniques of Femtosecond Time-Resolved Optical Polarigraphy (FTOP) combined with Induced Absorption (IA) microscopy with temporal and spatial resolutions equal to 450 fs and 2 μm, respectively. During the propagation of a pump pulse, its interaction with the target material is characterized by the breakup of the entire laser beam into separate filaments and the formation of non-stationary absorbing centers in their cores (probably laser-induced plasma that relaxes, by producing absorbing centers of different nature). Starting from delays of $\sim$ 300 ps, we observed the propagation of blast waves both in glass and in fused silica. Their propagation velocities have been directly measured.

1. Introduction

Investigations of the regularities characteristic of the propagation of powerful femtosecond pulses in transparent media are of considerable scientific and practical interest and represent one of the central problems of the new promising field – femtooptics of materials. It is known that, long before a laser pulse reaches the focus region, where the initial stage of the breakdown takes place, a high intensity of the electromagnetic wave field results in the initiation of the filamentation phenomenon practically in all transparent media from gases to solid bodies, i.e. one observes a breakdown of the entire beam into separate fine tracks, whose diameter (several microns in transparent dielectrics) conserves along many Rayleigh lengths. Recently, the filamentation has aroused a significant interest both due to the attractiveness of the complicated physical picture of this phenomenon for investigators and due to its practical importance [1]. The basic point in the filamentation process is the balance (dynamic and/or stationary) of the Kerr self-focusing and the plasma defocusing that restricts the former. There exist various models of filamentation (model of movable foci [2], self-channeling [3], dynamic [4,5], and X-wave models [6]). All of them describe certain aspects of this phenomenon, but, due to the complex nature of the formation and the maintenance of a filament, a complete physical model that covers all stages of filamentation is still absent. There are a number of problems concerning the regularities of the formation of filaments, mechanisms of their propagation, energy kinetics, and permanent modification of physical properties of the medium that explain the continuous interest in this phenomenon from both fundamental and practical viewpoints [1].

The given work is aimed at the creation of a new technique allowing one to study the regularities of the propagation of powerful femtosecond pulses in transparent media in real time and space. This technique is used for the determination of time intervals and mechanisms of various stages of the propagation of such pulses – from the Kerr self-focusing and the generation of plasma during the pulse propagation to specific channels of its energy relaxation that end with the formation of blast waves.

In this work, we used, for the first time, our microscopy techniques (FTOP and IA) as parts of a single

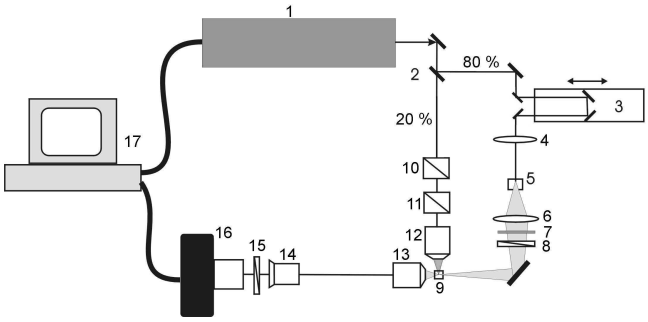

Fig. 1. Diagram of the experimental set-up: *1* – femtosecond regenerative amplifier Legend F-1k-He; *2* – splitting mirror; *3* – delay line; *4* – lens; *5* – medium for the generation of a white continuum; *6* – lens; *7* – optical color-glass filter; *8* – polaroid; *9* – sample under study; *10, 11* – Glan prisms; *12* – microscope objective ×10, numerical aperture 0.3; *13* – microscope objective ×10, numerical aperture 0.25; *14* – eyepiece ×15; *15* – polaroid; *16* – CCD-chamber; *17* – computer-aided measurement control system

complex, which allowed us to unite the pictures of the propagation of a pump pulse and the IA dynamics in space and time. The laser breakdown kinetics was studied in real time and space in the range of time delays varying from zero to 1.7 ns at a temporal resolution of 0.45 ps and a spatial one reaching 2 μm. The investigations were performed for model objects – samples of borosilicate K-8 optical glass (energy gap $E_g \sim 4$ eV [7]) and KU-1 fused silica (energy gap $E_g \sim 9$ eV [8]) produced in the form of polished bars $3 \times 3 \times 20$ mm in size.

2. Experiment

The diagram of the developed technique is illustrated in Fig. 1.

As an excitation source, we used a femtosecond complex with regenerative amplifier *1* (Legend F-1k-He) that provided the generation of single pulses with the following parameters: the pulse energy $W = 2.5$ mJ, duration $\tau_p = 150$ fs, and maximum wavelength $\lambda_{\max} = 780$ nm. The output radiation was split by mirror *2* into two components relating as 80 and 20%. The beam with a higher energy was used for the generation of probe radiation – "quasi-white" continuum. The possibility of variation of the time interval between the excitation and probe pulses in the range 0 – 1.7 ns with a step of 5 fs was realized with the help of delay line *3*. After passing the latter, the beam was focused in the bulk of bar *5* made of fused silica with a waist in the focus region of ~ 0.5 mm. The polarization of the continuum radiation was established at an angle of 45° to the vertical axis with the help of polaroid *8*. The initial duration of the continuum pulse practically coincided with that of the generating one. However, as such radiation propagated through the optical elements, the pulse spread due to the dispersion of their refractive indices. With regard for the spectral band of the RGB filters of a CCD chamber, for example for the "green" component (registered by "green" pixels of a CCD chamber), its duration amounted to ~ 300 fs. The radiation of the "quasi-white" continuum is collected by lens *6* and focused in investigated sample *9* $3 \times 3 \times 20$ mm in size. The rest of the laser radiation (not transformed into the "quasi-white" continuum) is cut off by light filter *7*. The other part of the radiation (20% of the initial energy of the beam) – a horizontally polarized excitation beam – is directed to Glan prism *10* established at an angle of 45° to the vertical. One more Glan prism *11* transmits only the vertically polarized component. After passing through two Glan prisms, the maximal energy of the laser pulse coming to objective *12* amounted to 160 μJ. Then the excitation pulse is focused with the help of objective *12* (×10, numerical aperture 0.3) in the bulk of the investigated transparent sample at depths of ~ 1.5 and 0.5 mm from the surfaces, through which one performs focusing and observations, respectively. The observation region in the neighborhood of the focal point was provided with the help of objective *13* (×10, numerical aperture 0.25). Its real image was additionally magnified by eyepiece *14* that formed a virtual image localized in infinity. This virtual image was registered in blue, green, and red light with the help of color CCD chamber *16*, whose objective was adjusted to infinity. The regenerative amplifier, delay line, and CCD chamber were controlled by means of a personal computer.

Now let us consider the concept of measurements in the FTOP mode. It is described in Fig. 2.

Due to the Kerr effect, the excitation wave firstly induces the optical axis parallel to the vector of electric field intensity of the excitation wave $\mathbf{E}_{\text{pump}}$ (along the OY axis) in the isotropic sample. The magnitude of the induced birefringence amounts to $n_e - n_0 = I_{\text{pump}} \cdot n_2$, where I_{pump} is the intensity of the excitation radiation, and n_2 is the nonlinear refractive index. The Kerr response time in glass (~ 1 fs) is practically instantaneous as compared to the duration of the used femtosecond pulse. Such a Kerr medium acts on the probe pulse with the polarization $\mathbf{E}_{\text{probe}}$ directed at an angle of 45° to the OY axis like a phase plate changing its polarization from the linear to the elliptical one. Thus, polaroid *15* crossed with respect to polaroid *8*, that sets the initial polarization of the probe pulse in the diagram presented in Fig.

1, analyzes the elliptically polarized probe beam with quasiwhite spectrum, by transmitting only the component with the polarization direction normal to $\mathbf{E}_{\rm probe}$. This component represents the FTOP signal.

If the phase shift appearing due to the anisotropy is small (as it is in the given experiment), the following expression is valid for the FTOP signal [9]:

$$I_{\rm FTOP} = \pi^2 d^2 n_2^2 I_{\rm pump}^2 I_{\rm probe}/\lambda_{\rm probe}^2,$$

where $d$is the length of interaction of the excitation and probe radiations, $I_{\rm probe}$ is the intensity of the probe radiation, whereas $\lambda_{\rm probe}$ stands for its wavelength. Thus, $I_{\rm FTOP}$ describes the instantaneous distribution of the excitation intensity. According to a more exact expression given in [10], the spatial distribution of the FTOP signal intensity represents a convolution of the probe signal and the squared integral of the excitation intensity along the direction of interaction Y: $\left(\int I_{\rm pump} dy\right)^2$. That is why, interpreting the FTOP image, one should take into account that the nonzero duration of the probe pulse results in the spreading of the image along the propagation axis similar to the softening of a moving object in a common photo in the case of a large exposition.

It is also worth noting that the axes of polaroids *8* and *15* in Fig. 1 are mutually perpendicular. By locating isotropic sample *9* between them, one observes the total blanking for the probe beam. If the axis of polaroid *15* is settled in parallel to that of polaroid *8*, then the set-up operates in the IA mode. That is, the IA picture is registered in the neighborhood of the focal point at various time delays $\tau_{\rm delay}$ between the excitation and probe pulses. If polaroid *15* is settled in the crossed position, then the set-up operates in the FTOP mode, by registering a temporary change of the induced anisotropic refractive index in the same spatial region. It is necessary to emphasize that the rotation of polaroid *15* does not change the temporal delay between the excitation and probe pulses, so one can obtain images both in the IA and FTOP modes for the same values of $\tau_{\rm delay}$.

It is also worth noting that, if the induced absorption takes place under the action of a pump pulse, it will be also observed in the FTOP mode. In essence, FTOP photos represent superpositions of FTOP proper and IA.

The created techniques allowed us to investigate the time and spatial kinetics of the laser breakdown in transparent media in the range of time delays from zero to 1.7 ns with a time resolution of 0.45 ps and a spatial one reaching 2 μm. The investigated samples were placed on a precision coordinate table. After each laser pulse, the sample was shifted by 50 μm so as the next pulse could act on a new region of the sample.

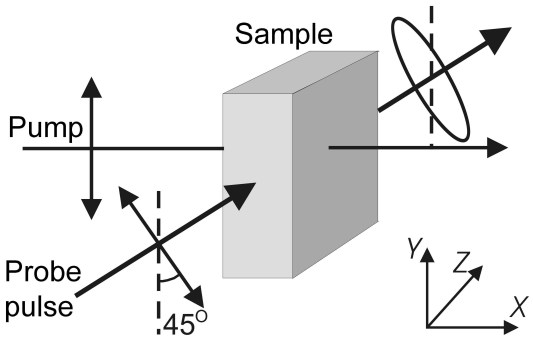

Fig. 2. FTOP concept. The excitation pulse polarized along the Y axis propagates along the X axis. The probe pulse polarized at an angle of 45° to the Y axis propagates along the Z axis

3. Results and Their Discussion

Let us consider the results of studying the processes caused by the propagation of femtosecond pulses in transparent media starting from those determined by the development of the Kerr nonlinearity and finishing with the laser breakdown of materials and the propagation of blast waves. First, we will analyze the results obtained at the shortest time intervals (0–1 ps) with the use of the above-described techniques for uniform samples made of K-8 glass in the single-pulse operation mode.

In Fig. 3, we present the photos (*a*–*e*) obtained in the FTOP (upper darker ones) and IA (lower lighter) geometries for several values of $\tau_{\rm delay}$ from the interval 0–1 ps at a pump beam energy of 160 μJ. The pulse propagates from the left to the right; the length of the registered propagation region is equal to 470 μm. The bright white strip in the focal region in the FTOP photos is evidently caused by the recombination radiation of the laser-induced plasma passing through polarizer *15*. The figure shows only the components of the whole color image corresponding to "green" pixels of a CCD chamber. One can see from the FTOP images that, at the initial stage of propagation ($\tau_{\rm delay} = 0$ ps (*a*)), the pulse is not yet filamented. However, at $\tau_{\rm delay} = 0.2$ ps (*b*), the filamentation is already observed in IA, whereas it is absent in FTOP. As $\tau_{\rm delay}$ increases up to 1 ps, the filamentation lines in IA intensify and appear in the FTOP images as well (also as the reabsorption of the probe radiation). In this case, one observes a convergence of the filaments in the direction of the focus, Fig. 3,*b*–*e*. The mean diameter of a filament amounts to $\sim$2 μm, its length exceeds 200 μm. In the neighborhood of the focal point, the FTOP signal abruptly decreases, probably due to the increasing IA of the probe radiation.

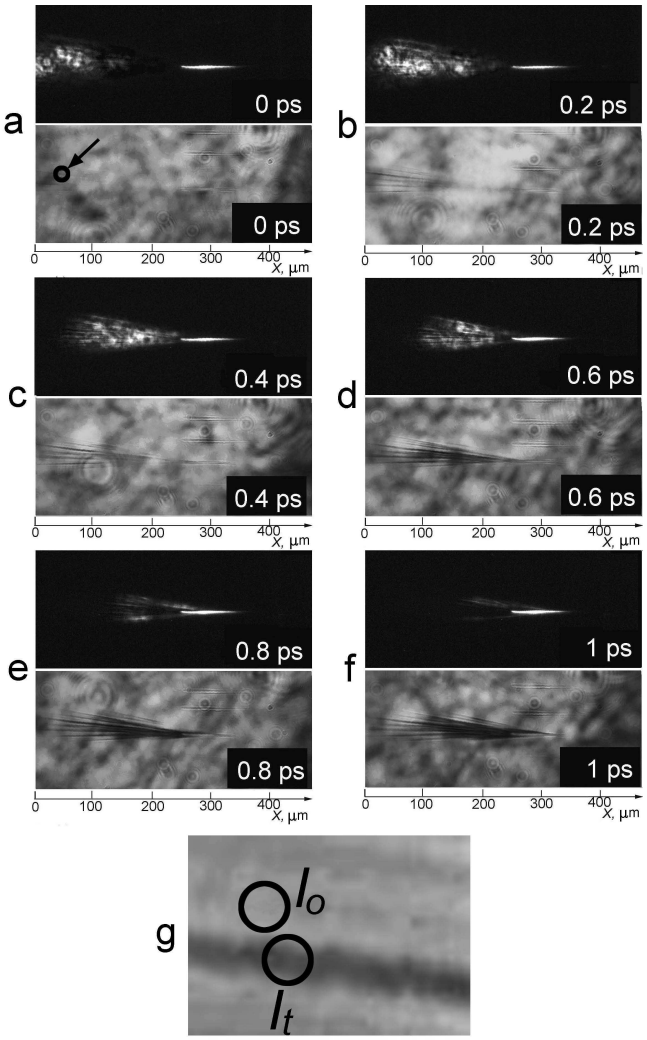

Fig. 3. Visualization of the propagation of a pump pulse in K-8 glass obtained by the FTOP technique and the corresponding IA images at the same time delays

It is worth paying attention to the fact that the width of the FTOP image along the X axis considerably exceeds the value derived from the duration of a laser pulse (equal to 150 fs) and the light propagation velocity in K-8 glass. This protraction is first of all caused by the dispersion of the optical elements, which results in the fact that, even within the spectral transmission band of the green light filter of a CCD chamber (∼70 nm), the short-wave component of the probe pulse is behind its long-wave component (chirp phenomenon). The time width $\Delta\tau$ of the "green" part of the excitation pulse along the X axis, that was estimated by the FTOP images with regard for the additional protraction due to the time of propagation of the probe beam through the region occupied by the excitation one, approximately amounts to 0.45 ps (the mean diameter of the excitation beam in the pre-focal region of the FTOP image is equal to ∼70 μm according to the data of Fig. 3,*b*). As was already mentioned, this value was accepted as the time resolution of the experimental set-up. As it represents the convolution of the 150-fs excitation pulse and the probe pulse, so the duration of the latter is close to 0.3 ps. One can see from Fig. 3 that the threshold of the IA appearance corresponds to the leading edge of the excitation pulse, while its maximal value is reached at the end of the pulse. In the IA photos, one can clearly distinguish about 10 filaments. Such a division of the initially integral beam into separate filaments in the case where the power of the excitation beam considerably exceeds the critical one is induced by the modulation instability [11]. Thus, we can suppose that each filament possesses ∼16 μJ of the energy of the excitation pulse. It is worth paying attention to the fact that, in the FTOP photos, the filamentation is less pronounced than that in IA. It testifies to the fact that the diameter of the localization region of the electromagnetic field of a laser pulse exceeds 2 μm, while the localized filament-like tracks are caused by IA. In the given stage, one can suppose that, at the beginning, IA is induced by plasma produced in the process of multiphoton nonlinear light absorption by the target material in the filament core, whereas, later on, it is caused by induced centers of other nature which are created in the process of relaxation of free carriers in the plasma and are characterized by a certain inertia of manifestation.

Figure 4 reflects the temporal IA dynamics in K-8 glass. The magnitude of absorption in the filament αd was calculated from the IA photos presented in the lower part of Fig. 3,*a–e* as $\ln(I_0/I_t)$, where I_t is the intensity of the signal quenched due to the absorption (grey level) that was measured in the middle of the filament image, and I_0 is that outside the filament but in its immediate vicinity. The measuring technique is explained in Fig. 3,*g*. It is possible only due to the reproducibility of the spatial structure of filaments from one pulse to another. The point of measurements marked by a circle in Fig. 3,*a* remained constant with varying delay time. Its coordinate ($X = 45$ μm) corresponds to the position of the maximum of the integral FTOP signal at $\tau_{\text{delay}} = 0$ ps. As the spatial scale of an inhomogeneity of the probe radiation considerably exceeds the filament diameter, the indicated measuring procedure can be considered correct. From Fig. 4, one can see that, as it was supposed, the absorption of the probe radiation starts at the lead-

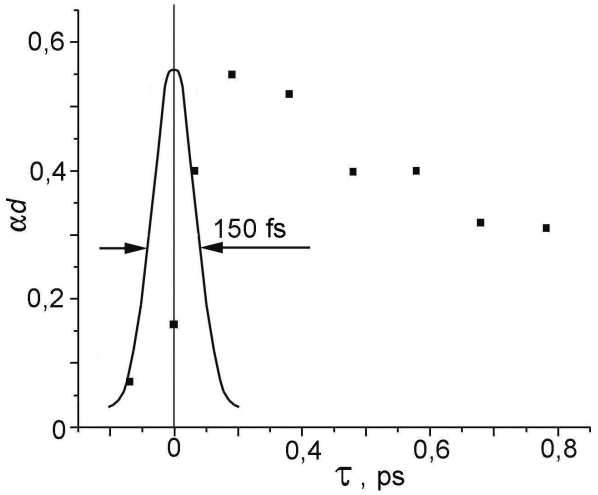

Fig. 4. Dots show the IA dynamics in K-8 glass at $X = 45$ μm. The shape of an excitation pulse is presented for comparison (solid line)

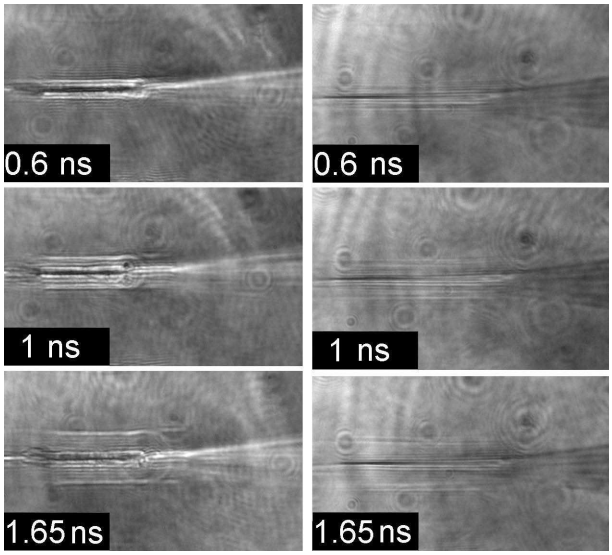

Fig. 5. Propagation of a sound wave from the breakdown region for different $\tau_{\rm delay}$. The length of each photo amounts to 120 μm. At the left – KU-1 fused silica, and at the right – K-8 glass. The values of $\tau_{\rm delay}$ are indicated in the photos

ing edge of the excitation pulse and reaches a maximum after its completion, which is followed by a decay determined by recombination processes. The measured rise time of absorption (~ 0.4 ps) exceeds the duration of a pump pulse $\tau_p = 150$ fs and is determined by the time resolution of the system.

Thus, the first stage of the interaction of a femtosecond pulse with the sample material is characterized by a decay of the integral laser beam into separate filaments caused by the so-called modulation instability and the formation of IA in the core of filaments.

Finally, in the case where the power of femtosecond pulses reaches critical values, the processes of energy relaxation of free carriers in transparent media are followed by the destruction of the sample. Without considering the complex nature of this process, we will analyze its kinetics. In this connection, let us consider Fig. 5 that demonstrates the IA pictures in the nanosecond scale of $\tau_{\rm delay}$. It is known that the process of material destruction is accompanied by the formation and the propagation of blast waves resulting in the intense compression of the substance and thus in the variation of the refractive index of the medium. We directly observed this process in the IA geometry in K-8 glass and in KU-1 fused silica at an energy of excitation pulses of 160 μJ.

It follows from the analysis of the obtained photos that, starting from $\tau_{\rm delay} \sim 300$ ps, we observed the separation of the blast wave front from the breakdown region in the both materials. Moreover, in addition to the propagation of a cylindrical wave from the focal line, one can observe the propagation of a spherical wave from the point of the maximal energy release in silica. With increasing $\tau_{\rm delay}$, the diameter of the wave linearly rises in proportion to the speed of sound propagation in the investigated materials V_s. The values of V_s determined by the data of Fig. 5 appeared to be equal to 6.8 ± 0.4 km/s for K-8 glass and 6.0 ± 0.3 km/s for KU-1 fused silica, which agrees with the tabular data.

4. Conclusions

We have studied the basic stages of the propagation of a femtosecond laser pulse in optical glass and fused silica. The investigations were performed with the use of the developed microscopy FTOP and IA techniques. Due to their complex application, we managed for the first time to unite the pictures of the propagation of a pump pulse and the IA dynamics in time and space. On the first stage, the propagation of a femtosecond pulse is characterized by the decay of an integral laser beam into separate filaments and the formation of absorbing centers (possibly, a laser-induced plasma that relaxes, by producing absorbing centers of different nature) in their core during the propagation of the pump pulse. The second stage of the interaction that starts from delays of $\sim$300 ps both in glass and in fused silica is characterized by the initiation of irreversible changes in the focal region and the propagation of blast waves. The speeds

of their propagation were determined by direct observations.

The work was performed with the methodical support of the NASU Center for Collective Use of Equipment "Laser Femtosecond Complex" and the partial financial support by grants No. F17/45-2007 of the FRSF of the Ministry of Education and Science of Ukraine and No. 3745 of the Science and Technology Center in Ukraine.

The authors express sincere thanks to the collaborators of the CCUE "Laser Femtosecond Complex" I.M. Dmytruk and P.I. Korenyuk for their help in the investigations.

1. A. Couairon and A. Mysyrowicz, Phys. Rep. **441**, 47 (2007).
2. V.N. Lugovoi and A.M. Prokhorov, Pis'ma Zh. Eksp. Teor. Fiz. **7**, 153 (1968).
3. A. Braun, G. Korn, X. Liu, D. Du, J. Squier, and G. Mourou, Opt. Lett. **20**, 73 (1995).
4. M. Mleinek, E.M. Wright, and J.V. Moloney, Opt. Lett. **23**, 382 (1998).
5. V.P. Kandidov, O.G. Kosareva, and A.A. Koltun, Kvant. Elektr. **33**, 69 (2003).
6. M. Kolesik, E.M. Wright, and J.V. Moloney, Phys. Rev. Lett. **92**, 2539011-4 (2004).
7. A. Horn, E.W. Kreutz, and P. Poprawe, Appl. Phys. A **79**, 923 (2004).
8. A. Zoubir, C. Rivero, R. Grodsky, K. Richardson, M. Richardson, T. Cardinal, and M. Couzi, Phys. Rev. B **73**, 224117 (2006).
9. J. Takeda, K. Nakajima, S. Kurita, S. Tomimoto, S. Saito, and T. Suemoto, Phys. Rev. B **62**, 10083 (2000).
10. M. Fujimoto, S. Aoshima, M. Hosoda, and Y. Tsuchiya, Phys. Rev. A **64**, 033813 (2001).
11. A.J. Campillo, S.L. Shapiro, and B.R. Suydam, Appl. Phys. Lett. **23**, 628 (1973).

Received 05.02.09.
Translated from Ukrainian by H.G. Kalyuzhna

ПРЯМЕ СПОСТЕРЕЖЕННЯ ЕТАПІВ ЛАЗЕРНОГО РУЙНУВАННЯ ЗРАЗКІВ ПРОЗОРИХ МІШЕНЕЙ У ЧАСОВОМУ ДІАПАЗОНІ ВІД ФЕМТО- ДО НАНОСЕКУНД

І.В. Блонський, В.М. Кадан, О.Й. Шпотюк, І.А. Павлов

Р е з ю м е

З використанням створених методик фемтосекундної часороздільної оптичної поляриграфії (ФЧОП) у поєднанні з мікроскопією індукованого поглинання (ІП) з часовою роздільною здатністю 450 фс і просторовою – 2 мкм досліджено основні стадії лазерного руйнування та явища, які їх супроводжують, при дії потужних фемтосекундних імпульсів на типові ізотропні прозорі середовища: оптичне скло К-8 і плавлений кварц КУ-1. Вже під час проходження імпульсу накачки його взаємодія з матеріалом мішені характеризується розпадом суцільного лазерного променя на окремі філаменти і формуванням в їхньому ядрі нестаціонарних поглинаючих центрів (імовірно лазерно-індукованої плазми, яка релаксує з утворенням поглинаючих центрів іншої природи). Починаючи із затримок ~ 300 пс як в склі, так і в плавленому кварці, спостерігається поширення ударних хвиль. За прямими спостереженнями визначено швидкості їх поширення.